Heliyon 6 (2020) e05591

Contents lists available at ScienceDirect

Heliyon

journal homepage: www.cell.com/heliyon

Research article

Gold nanoparticles carrying or not anti-VEGF antibody do not change glioblastoma multiforme tumor progression in mice

Viviane de Cassia Jesus da Silva [a], Renee de Nazare O. Silva [c], Lucas Giglio Colli [b], Maria Helena Catelli de Carvalho [b], Stephen Fernandes Rodrigues [a,b,*]

[a] Laboratory of Vascular Nanopharmacology, Department of Pharmacology, Institute of Biomedical Sciences I, University of Sao Paulo, Sao Paulo, SP, Brazil
[b] Laboratory of Hypertension, Diabetes and Vascular Biology, Department of Pharmacology, Institute of Biomedical Sciences I, University of Sao Paulo, Sao Paulo, SP, Brazil
[c] Department of Pharmacology, Institute of Biomedical Sciences I, University of Sao Paulo, Sao Paulo, SP, Brazil

ARTICLE INFO

Keywords:
Metallic nanoparticles
Brain cancer
Growth factor
Rodents
VEGF
Systems biology
Cancer research
Chemotherapy
Pathophysiology
Pharmacology
Oncology

ABSTRACT

Aims: Glioblastoma multiforme (GBM) is the most devastating malignant primary brain tumor known. Life expectance is around 15 months after diagnosis. Several events contribute to the GBM progression such as uncontrolled genetic cancer cells proliferation, angiogenesis (mostly vascular endothelial growth factor (VEGF)-mediated), tissue invasion, glioma stem cell activity, immune system failure, and a hypoxic and inflammatory tumor microenvironment. Tumor cells antiproliferative effect of 20 nm citrate-covered gold nanoparticles (cit-AuNP) has been reported, along with anti-inflammatory and anti-oxidative effects. We aimed to test whether either chronic treatment with 20 nm cit-AuNP or anti-VEGF antibody (Ig)-covered AuNP could reduce GBM progression in mice.

Main methods: Effect of the gold nanoparticles on the GL261 glioblastoma cells proliferation *in vitro*, and on the GL261-induced glioblastoma cell growth in C57BL/6 mice *in vivo* were tested. Besides, fluorophore-conjugated gold nanoparticles penetration through the GL261 plasma cell membrane, gold labelling in brain parenchyma of glioblastoma-carrying mice, and VEGF expression into the tumor were evaluated.

Key findings: We observed cit-AuNP did no change the GL261 cells proliferation. Similarly, we demonstrated chronic treatment with either cit-AuNP or anti-VEGF Ig-covered AuNP did not modify the GL261 cells-induced GBM progression in mice. By the end, we showed AuNPs did not trespass in appreciable amount both the GL261 plasma cell membrane and the tumoral blood brain barrier (BBB), and did not change the VEGF expression into the tumor.

Significance: 20 nm cit-AuNP or anti-VEGF Ig covered-AuNP are not good tools to reduce GBM in mice, probably because they do not penetrate both tumor cells and BBB in enough amount to reduce tumor growing.

1. Introduction

Glioblastoma multiforme (GBM) is the most aggressive form of primary brain malignant tumor and the most common one, accounting for 48% of all malignant central nervous system (CNS) tumors [1]. It reaches people around 60 years old but can occur at any age [for revision, [2, 3, 4, 5]]. Therapeutic strategies such as chemotherapy (using more frequently temozolomide), radiotherapy and surgical resection can be used, although GBM recurrence is frequently observed. In fact, the overall survival in affected people is around 15 months and the overall 5-year survival is less than 5% [6, 7]. Then, a search for a more effective treatment is mandatory.

GBM physiopathology involves uncontrolled genetic cancer cells proliferation, angiogenesis, tissue invasion, glioma stem cell activity, immune system failure in recognizing cancer cells and a hypoxic and inflammatory tumor microenvironment [8, 9]. Regarding to the GBM inflammation, cells like microglia, infiltrating macrophages, T-lymphocytes, non-neoplastic astrocytes and mast cells, cytokines such as transforming growth factor-beta (TGF-β), interleukin 6 (IL-6), interleukin 8 (IL-8) and tumor necrosis factor-alpha (TNF-α), and transcription factors

* Corresponding author.
E-mail address: stephen.rodrigues@usp.br (S.F. Rodrigues).

https://doi.org/10.1016/j.heliyon.2020.e05591
Received 11 July 2020; Received in revised form 20 August 2020; Accepted 19 November 2020

Table 1. The gold nanoparticles features.

Features/Nanoparticle types	cit-AuNP	Anti-VEGF Ig-covered AuNP	DY654-AuNP
Average size (nm)	20.1 ± 2.4	-	-
Hydrodynamic diameter (DLS) (nm)	22.9 ± 3.7	39.0 ± 3.4	37.8 ± 2.1
Zeta potential (mV)	-26.1 ± 0.5	-8.02 ± 0.3	-6.4 ± 0.5
pH	5	5	7.5
Concentration (nanoparticles/mL)	1.9×10^{12}	1.9×10^{12}	1.9×10^{12}
Peak SPR wavelength (nm)	522	527	527

Data provided by the manufacturer (Nitparticles Company, Zaragoza, Spain).

such as nuclear factor-kappa B (NF-κB), all contribute in different ways to tumor progression [10].

Another important player for the GBM progression is the vascular endothelial growth factor (VEGF), which is over-expressed by GBM cancer cells, mainly glioma stem cells (GSC) under hypoxia, and contributes to tumor development by inducing neovascularization [11]. In fact, GBM is a highly vascularized tumor [12]. GSC are present in low amount into the tumor, however, they are essential for tumor progression once these cells are self-renewing, show resistance to radiotherapy and chemotherapy, *in vitro* differentiate into other cell types, and are greatly responsible for tumor recurrence [13]. The tumor vascularization is immature, disorganized, and usually partially thrombus occluded though [11]. Fluid can easily trespass the blood brain barrier (BBB) and leads to cerebral edema, which highly influences tumor progression and symptoms [14].

Nanodrugs are an exciting therapeutic tool and some therapies containing those drugs have been marketed the last two decades. They are used to treat different diseases, such as infections, some cancers, inflammation, and others (for revision, [15, 16, 17, 18, 19]).

As nanoparticles, the gold ones (AuNP) reunite several desirable features. They are easy to prepare, biocompatible, easy to obtain a specific size nanoparticle and to conjugate with a variety of molecules, including, drugs and antibodies. Besides, AuNPs own a special property, which is called surface plasmon resonance (SPR). The SPR enables the AuNP to absorb light and convert it into heat. Thus, hyperthermic therapy can be performed using AuNP [20]. Furthermore, we demonstrated that 20 nm citrate-covered AuNP (cit-AuNP) can reduce *in vivo* leukocyte adhesion to endothelial cells in surgery-stimulated mesenteric vessels of Wistar rats [21].

Taking the inflammatory microenvironment of the GBM into account, strategies to reduce its effects may be of great importance to prevent the full GBM progression. In fact, reduction of microglia/macrophage influence on the GBM after peptide R use, an antagonist of the chemokine receptor CXCR4, or K-rhein inhalation, a CD38 inhibitor, in tumor-bearing mice showed great reduction of tumor volume [22, 23]. Although the mechanism by which gold nanoparticles interfere with the leukocytes function in cancer is largely unknown, whether gold nanoparticles could impair the immunosuppressive leukocytes, they would be beneficial for reducing the GBM growth. Besides, a reactive oxygen species (ROS)-rich microenvironment favors a series of epigenetic alterations that further support the GBM progression, for example, changes in the deoxyribonucleic acid (DNA) methylation and acetylation of histones, with consequent DNA repair enzymes malfunctioning [24, 25]. Once some studies have demonstrated an antioxidative effect of 20 nm citrate-covered gold nanoparticles, they could potentially reduce the GBM growing [26, 27]. Furthermore, it was reported that gold nanoparticles reduce tumor cells proliferation, enhances caspase 3 and 8 expressions, and reduces Bcl-2 and the mitogen-activated protein kinase/extracellular signal-regulated kinase (MAPK/ERK) expressions [28, 29]. Caspases 3 and 8 are proapoptotic enzymes, Bcl-2 modulates the proapoptotic effects of caspases, and MAPK/ERK signaling play important roles in the following processes: cell growth, proliferation, differentiation, migration and apoptosis, all of them are important for tumor progression [30, 31, 32]. However, whether 20 nm citrate-covered gold nanoparticles can inhibit the GL261 cells proliferation and tumor progression remains largely unknown.

Regarding to the chemotherapy, besides temozolomide, the standard drug used to treat GBM and that increases in some months the median survival [7], VEGF antibody (Ig) (bevacizumab) was approved by the Food and Drug Administration (FDA) agency in USA and is the only drug used today in recurrent GBM [33]. Unfortunately, its effects in GBM are noticeably short. Part of the transient action of bevacizumab is supposed to come of bevacizumab targets only the circulatory VEGF, but not the VEGF located in the brain parenchyma. Free antibodies do not cross the BBB, and transport through the BBB using virus, nanocarriers and local delivery promises to be excellent strategies to overcome that drawback [34, 35, 36]. In this way, whether an anti-VEGF Ig-covered gold nanoparticle can reduce GBM progression in mice remains elusive.

Then, in this paper we aimed to test whether chronic 20 nm cit-AuNP or an anti-VEGF Ig-covered AuNP treatment could reduce the GBM progression in mice. We found that neither 20 nm cit-AuNP or an anti-VEGF Ig-covered AuNP changed the GL261-cells induced GBM volume in mice, probably by not trespassing in enough amount either the tumor cell plasma membrane or the BBB.

2. Material and methods

2.1. Gold nanoparticles (AuNP)

All gold nanoparticles used in this study were ordered from the Nitparticles Company (Zaragoza, Spain) and their features are showed in the Table 1 below. Citrate (cit)-AuNP were diluted in Milli-Q H_2O, citrate used to stabilize the gold nanoparticles in solution, avoiding aggregates formation and, then, changes in nanoparticles diameter. Cit-gold nanoparticles stability is one year, according to the manufacturer. The anti-VEGF Ig-covered AuNP were prepared by previously conjugating the 20 nm cit-AuNP with 5 kDa polyethylene glycol-(PEG) COOH and their further functionalization with the low endotoxin and azide free anti-mouse VEGF-A monoclonal Ig (catalog #512808, Biolegend, CA, USA). The conjugated anti-VEGF Ig gold nanoparticles were diluted in 10 mM 2-(N-morpholino)ethanesulfonic acid (MES). According to the vendor, the binding between gold nanoparticles and antibodies is high and the bond is stable, it is performed in the Fc region of the antibody, leaving the antibody Fab region available for binding the antigen. The bioconjugate stability will depend on the long-term stability of the antibody itself against degradation. Bioconjugation was confirmed as demonstrated in the Table 1 below and supplementary material. Antibody functional activity after gold nanoparticle bioconjugation was also confirmed as demonstrated in the supplementary material. The DY654-AuNP were previously prepared by conjugating the 20 nm cit-AuNP with 5 kDa polyethylene glycol-(PEG)COOH and their further functionalization with the fluorophore DY-654. The conjugated DY654 gold nanoparticles were diluted in phosphate buffered saline (PBS) 1x.

2.2. GL261 cell culture

The murine glioblastoma cell culture lineage GL261 was purchased from the Banco de Células do Rio de Janeiro (Rio de Janeiro, Brazil). The GL261 cells were maintained in the RPMI 1640 cell media (Cultilab, Sao Paulo, Brazil), supplemented with 10% heat inactivated fetal bovine serum (FBS) (Vitrocell, Sao Paulo, Brazil) in a humidified CO_2 incubator, containing 5% CO_2 and at 37 °C.

2.3. GL261 cell growth curve

The effect of cit-AuNP on the GL261 cell proliferation was tested. To perform that, the GL261 cells were seeded on a 24-well plate (1×10^4 cells/well). Twenty-four hours later, the cells were placed in contact with the following serial dilution of cit-AuNPs: 0.01%, 0.03%, 0.1%, 0.3%, 1%, or RPMI medium, and GL261 count in each well was performed 24, 72 and 96h later, using a hemocytometer. Medium containing or not the cit-AuNP was replaced every 48 h. A 0.05% trypsin/EDTA solution (Cultilab, Brazil) was used to cover the cell monolayer in each well to detach the cells just before counting. It was followed a centrifugation (3000x rpm), dispersion in 1 mL of RPMI medium and Trypan blue (10:1, vol:vol) (Sigma-Aldrich, St. Louis, MO, USA), and count.

2.4. Animals

Seven-week-old female C57BL/6J mice (18–22 g body weight) were purchased from the Facility for specific-pathogen-free (SPF) mice production at University of Sao Paulo (USP) Medical School Animal Facility Network at USP. They were kept in the mice vivarium of the Pharmacology Department in the Institute of Biomedical Sciences (IBS) until use. Mice were housed under specific pathogen free conditions, controlled room temperature (22–24 °C) and humidity (40–80%). They were fed chow and water *ad libitum* till use. All experimental procedures involving animals performed in this study were previously approved and certified (#060/2015) by the Ethical Committee for Animal Usage of IBS (called CEUA-ICB), which follows rules determined by the National Council for Experimental Animal Controlling (called CONCEA, Brazil) and the National Institutes of Health (NIH) guide for the care and use of Laboratory animals. All efforts were made to reducing suffering.

2.5. In vivo tumor induction

GBM was *in vivo* induced in 8- to 10-week-old female C57BL/6J mice by injecting 1×10^5 GL261 cells into the brain parenchyma. Animal species and lineage were chosen based on the immune system integrity for the GBM model we used, our previous experience, and reliability of the results [37]. Briefly, mice were intraperitoneally (IP) anesthetized with a solution containing ketamine and xylazine (100 mg/kg and 10 mg/kg body mass, respectively). Mice were then positioned in an acrylic plaque in a sphinx pose and a vertical incision was performed in the skin to expose the skull. Using an electrical drill, a 2 mm hole was done in the skull, 1 mm to the right of the sagittal suture and 1 mm posterior to the coronal suture. Through the hole and using a 10 μL Hamilton syringe and a 26G needle attached, 1×10^5 GL261 cells dispersed in 2 μL RPMI cell medium without FBS were injected 2.7 mm to the right of the sagittal suture, 0.5 mm posterior to the coronal suture and 2.4 mm deep into the cerebral parenchyma over 8 min. To do that, an automated microinjection system attached to a motorized stereotaxic device was used (Neurostar, Sindelfingen, Germany). Needle was kept in position into the tissue for 10 min after injection. The original skull bone was placed back and fixed with bone cement (Fillcanal®, Technew, Rio de Janeiro, RJ, Brazil). Nylon 6-0 suture (Shalon, Goiania, GO, Brazil) was used to close the incision and 2 mg/kg body mass ketoprofen (Biofen®, Biofarm, Jaboticabal, SP, Brazil) was IP injected by the end of the surgical procedure in order no alleviate pain. All surgery was done under sterile operating room condition.

2.6. Chronic treatment with gold nanoparticles

Eight days after GBM induction in mice, 1×10^{11} cit-AuNP, 1×10^{11} anti-VEGF Ig covered-AuNP, anti-VEGF Ig, or saline were randomly intravenously (IV) injected (in a volume of 100 μL) in the femoral vein of mice once every three days up to the 25th day after GBM induction, performing then six shots. Alternate femoral vein was used at each time. To access the femoral vein, a small incision was performed in the skin under anesthesia with 4% isoflurane (Isoforine®, Cristalia, Itapira, SP, Brazil). After injection, nylon 6-0 suture was used to close the incision. The whole procedure lasted 15 min. Aseptic conditions were performed during the injection process. In a parallel study performed in our lab, the same dose of cit-AuNP (1×10^{11} nanoparticles) was seen to dramatically reduce inflammation in brain of sepsis-induced female mice the same age used in this study (unpublished results). Anti-VEGF Ig (used as control) was injected the same amount (8.9 mg/kg body weight) present in the 1×10^{11} anti-VEGF Ig covered-AuNP (according to the manufacturer, there was 5.6 anti-VEGF Ig molecules per AuNP).

2.7. Tumor volume, body weight and chow intake measurements

Twenty-five days after the GBM induction, mice were weighed, anesthetized using a ketamine/xylazine solution (100 mg/kg and 10 mg/kg body mass, respectively), a transcardial perfusion with 1x PBS was performed and brain was removed. An acrylic apparatus (World Precision Instruments, Sarasota, FL, USA) was used to cut the brain in 2-mm coronal slices to determine the tumor volume. The 2-mm slices were digitalized using a scanner (Epson Stylus TX235W, Manaus, AM, Brazil) and the total tumor areas were quantified using the Image J software (Image J 1.47v, NIH, USA). Tumor volume was expressed as percentage of the ipsilateral hemisphere. Tumors were frozen and kept in -80 °C freezer until use. Chow intake was measured 24 h before brain collection and expressed as g/24 h/kg body mass.

2.8. GL261 cell uptake of gold nanoparticles

To visualize the uptake of the AuNP by the GL261 cells, we used DY654-AuNP, which are fluorescent AuNP emitting light in the wavelength of 654 nm GL261 cells (the total number of 2×10^6) were seeded in a 12-well plate and 48 h later 10% DY654-AuNP were added into the wells. Cells were washed three times with 1x PBS 20, 40, 60 and 120 min following the DY654-AuNP incubation, RPMI medium was added in each well and AuNP cell uptake was quantified by confocal fluorescent microscopy (Axiovert 100M, ZEISS). Result was expressed as percentage of cells in each field containing a red fluorescence.

2.9. Measurement of gold nanoparticles in the cerebral parenchyma

Tumor-containing brains collected from twenty-five-day GBM-carrying mice 24h after the last i.v. chronic injection with either cit-AuNP or saline were incubated in 4% paraformaldehyde for 24h, followed by another 24h incubation with 30% sucrose solution, and tissue blocked using OCT® tissue freezing media (Tissue-Tek®, Sakura, Alphen aan den Rijn, the Netherlands). Tissues were kept at -80 °C freezer until usage. Ten millimeters brain cross sections were obtained using cryostat (Leica CM 1850, Heidelberg, Germany), they were fixed in glass slides previously coated with a thin layer of poly-L-lysine solution (Sigma-Aldrich, USA), put in contact with 1x PBS containing 0.3% Tween 20 (Sigma-Aldrich, USA) for 10 min, and gold presence was quantified using the commercially available kit GoldEnhance (Nanoprobes, Yaphank, NY, USA), following the manufacturer protocol. As positive control, cit-AuNP disposed in a glass slide were used, and as negative control, ultrapure water. Black labeling was characteristic of gold presence and visualized by light microscopy.

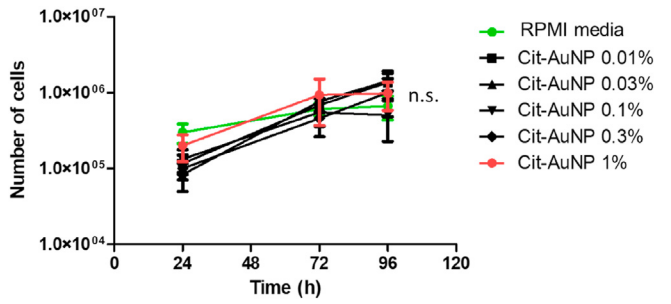

Figure 1. Effect of the citrate-covered gold nanoparticles (cit-AuNP) on the GL261 glioblastoma cells growth curve. Cit-AuNP in different concentrations (0.01%, 0.03%, 0.1%, 0.3%, or 1%) dissolved in culture medium or culture medium alone (control group) were incubated along with the glioblastoma GL261 cells for up to 96h. Number of GL261 cells were counted 24, 72 and 96h after cit-AuNPs incubation or cell culture medium incubation. No difference was observed after incubation with cit-AuNP compared to the control group ($P > 0.05$). Results are average of five different assays. Not significant, n.s.

2.10. Western blotting

Frozen cerebral tumor was powered, homogenized in lysis buffer (10% RIPA buffer, Merk Millipore, MA, USA), added 1 mM phenylmethylsulfonyl fluoride (PMSF) (Amresco, Solon, OH, USA), 10 mM sodium orthovanadate (Sigma-Aldrich), 100 mM sodium fluoride (LabSynth, Diadema, SP, Brazil), 10 mM sodium pyrophosphate (Sigma-Aldrich), and 0.2% protease inhibitor (P8340, Sigma-Aldrich), for 30 min at 4 °C, and centrifuged (15.000x g, 4 °C, 20 min) to obtain supernatant. Total proteins were quantified in supernatant (PierceTM BCA Protein Assay Kit, ThermoFisher Scientific), samples treated with Laemmli's buffer containing 350 mM dithiothreitol, and 50 μg of proteins were loaded on a 15% polyacrylamide gel (Sigma-Aldrich) and transferred to a polyvinylidene fluoride membrane (PVDF) (Amersham Hybond-P, GE Healthcare Life Sciences, UK) for 40 min, 80V and 4 °C. Nonspecific binding was blocked using 3% BSA in tween Tris buffered saline (TTBS) buffer (pH 7.6) (LabSynth) for 1 h, at room temperature. Membranes were incubated overnight with anti-VEGF-A primary antibody (1:500, vol:vol, Biolegend, CA, USA) diluted in blocking solution, at 4 °C. Beta-actin labeling (1:5,000, vol:vol, Abcam, Cambridge, MA, USA) after membrane stripping (Restore™ Western Blot Stripping Buffer, Thermo Fisher Scientific) was used as loading control and results were related to it. HRP-conjugated secondary antibody (1:5,000, vol:vol, Santa Cruz Biotechnology) was incubated with the membrane for 1 h, at room temperature, blotting was visualized after incubation with a quimoluminescence solution (Pierce® ECL Western Blotting Substrate, Thermo Fisher Scientific), and images captured using a luminescence reader device (Carestream Molecular Imaging, Gel Logic 2200 PRO, Carestream Health, NY, EUA). Blotting density was quantified using the software Image J (Wayne Rasband), and expressed as arbitrary units.

2.11. Statistical analysis

All results are expressed as mean ± standard error of the mean (SEM). To verify whether there was difference between groups, unpaired student t-test or one-way ANOVA followed by Tukey test were used. All analyses were performed using the Prism 5 software (GraphPad Software, Inc.), and statistical significance was set as $P < 0.05$.

3. Results

3.1. Gold nanoparticles did not change the GL261 cell proliferation

Initially, we determined whether cit-AuNP could or not interfere with the GL261 cell proliferation, *in vitro*. We observed that none of the cit-AuNP concentration (0.01%, 0.03%, 0.1%, 0.3%, or 1%) tested

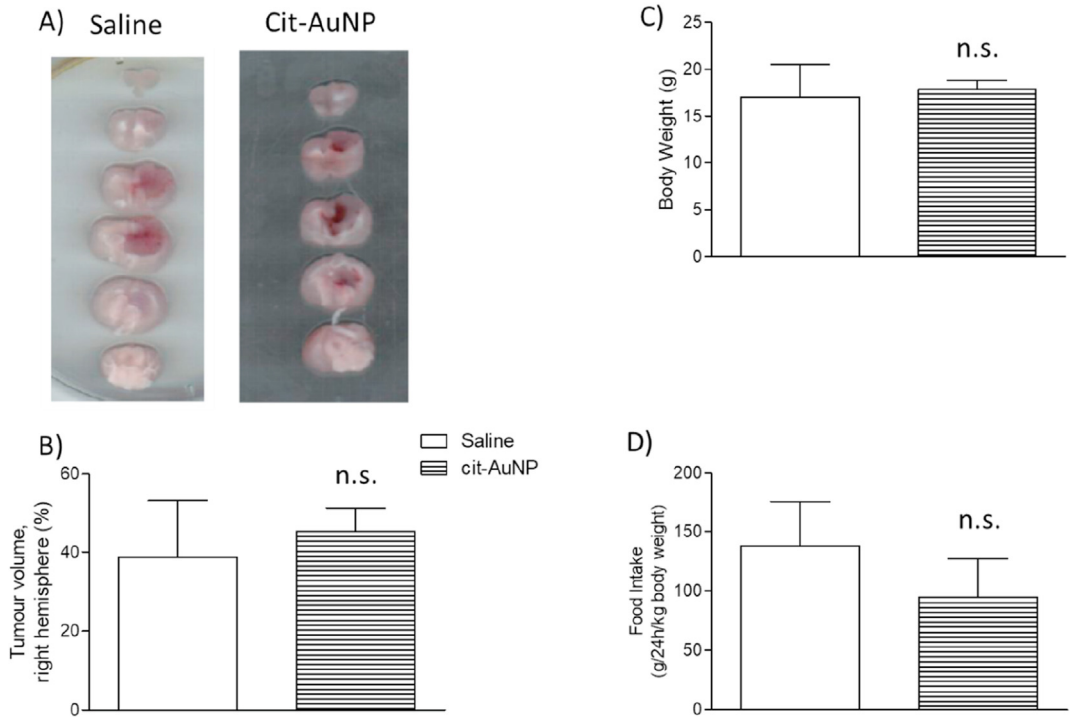

Figure 2. Effect of citrate-covered gold nanoparticles (cit-AuNP) on the GL261 cells-induced glioblastoma multiforme (GBM) progression in mice. A) Representative 2 mm-cerebral sections of the GBM-carrying mice intravenously and chronically treated with cit-AuNP or saline (control group) from day 8 up to day 25 after GBM induction, injected once every three days. GBM is darker than the health tissue. Tumor volume quantification (B), body weight (C) and food intake (D) of the 25-day-GBM-carrying mice chronically treated with cit-AuNP or saline. No difference was observed in the tumor volume, body weight and food intake after cit-AuNP treatment compared to the control group ($P > 0.05$). Three to four animals per group were tested and comparison was made by using unpaired t-test. Not significant, n.s.

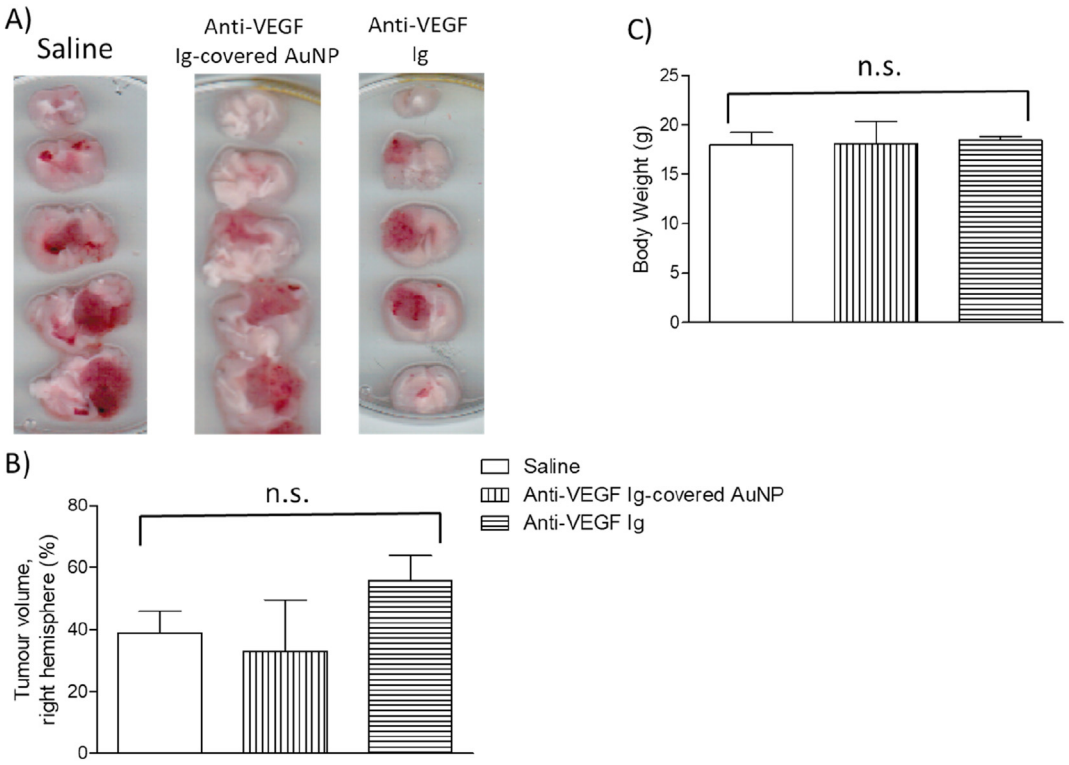

Figure 3. Effect of anti-VEGF antibody (Ig)-covered gold nanoparticles on the GL261 cells-induced glioblastoma multiforme (GBM) progression in mice. A) Representative 2 mm-cerebral sections of the GBM-carrying mice intravenously and chronically treated with anti-VEGF Ig-covered-AuNP, anti-VEGF Ig or saline (control groups) from day 8 up to day 25 after GBM induction, injected once every three days. GBM is darker than the health tissue. Tumor volume quantification (B), and body weight (C) of the 25-day-GBM-carrying mice chronically treated with anti-VEGF Ig-covered AuNP, anti-VEGF Ig or saline. No difference was observed in both the tumor volume and the body weight after anti-VEGF Ig-covered AuNP or anti-VEGF Ig treatment compared to the control group ($P > 0.05$). Three animals per group were tested and comparison was made by using ANOVA. Not significant, n.s.

changed the GL261 growth curve measured along 96h after cit-AuNP incubation (Figure 1).

3.2. Tumor volume was not changed after gold nanoparticles treatment

Chronic treatment with cit-AuNP did not change the tumor volume of GBM-carrying mice compared with the control group (treated with saline) (Figure 2A, B). The same way, chronic treatment with cit-AuNP did not modify both the body weight (Figure 2C) and the food intake (Figure 2D) measured 25 days after the GBM induction.

Performing another strategy, we tested whether anti-VEGF Ig-covered AuNP could reduce the GBM progression in mice. We observed anti-VEGF Ig covered-AuNP did not reduce GBM volume in mice (Figure 3A, B). Similarly, anti-VEGF Ig the same amount present in the anti-VEGF Ig covered-AuNP was injected in mice and did not change the GBM volume (Figure 3A, B). Anti-VEGF Ig covered-AuNP or anti-VEGF Ig did not reduce both the body mass of GBM-carrying mice (Figure 3C) and the amount of clotted blood vessels in the tumor (supplemental figure), measured 25 days after tumor induction.

3.3. Gold nanoparticles were not uptaken by the GL261 cells

Once it was previously demonstrated gold nanoparticles can modify some cellular processes, such as signaling pathways, intracellular ROS concentration and proteins expression [26, 27, 28], we verified whether AuNPs were uptaken or not by the GL261 tumor cells in an attempt to explain why no change in tumor volume was observed after chronically treating mice with cit-AuNP. To measure the traffic of gold nanoparticles through the GL261 cell membrane, we used fluorescent gold nanoparticles (DY654-AuNPs). We incubated GL261 cells in presence of the DY654-AuNP for 20, 40, 60 and 120 min. It was not observed any important DY654-AuNP uptake by the GL261 cells in any time tested compared with the control group (not incubated with DY654-AuNP) (Figure 4).

3.4. Gold was not found in the cerebral parenchyma of gold nanoparticles chronically treated GBM-carrying mice

We tested whether gold nanoparticles trespassed the BBB of the GBM-carrying mice by measuring gold in their cerebral parenchyma. We found no detectable gold both in the tumor and peritumoral areas of chronically treated GBM-carrying mice (Figure 5).

3.5. Anti-VEGF Ig-covered AuNP chronic treatment did not change the VEGF expression in the cerebral GBM tumor of mice

We measured the VEGF expression in the GBM tumor in brain of mice previously treated with anti-VEGF Ig-covered AuNP and we demonstrated VEGF concentration did not significantly changed compared to mice treated with saline (control) (Figure 6). Similarly, no difference in the VEGF expression into the tumor was observed in mice chronically treated with the anti-VEGF neutralizing antibody (Figure 6).

4. Discussion

In this paper, we showed that cit-AuNP or anti-VEGF Ig covered-AuNP did not reduce GBM progression in mice probably by not crossing in enough amount both the GL261 tumor cell membrane and the BBB.

Initially, we tested the effect of cit-AuNP on the GL261 glioblastoma cell line growth curve. We observed that 20 nm cit-AuNP, in different concentrations, did not change the GL261 proliferation status. Similar results were observed by other authors using different glioma/

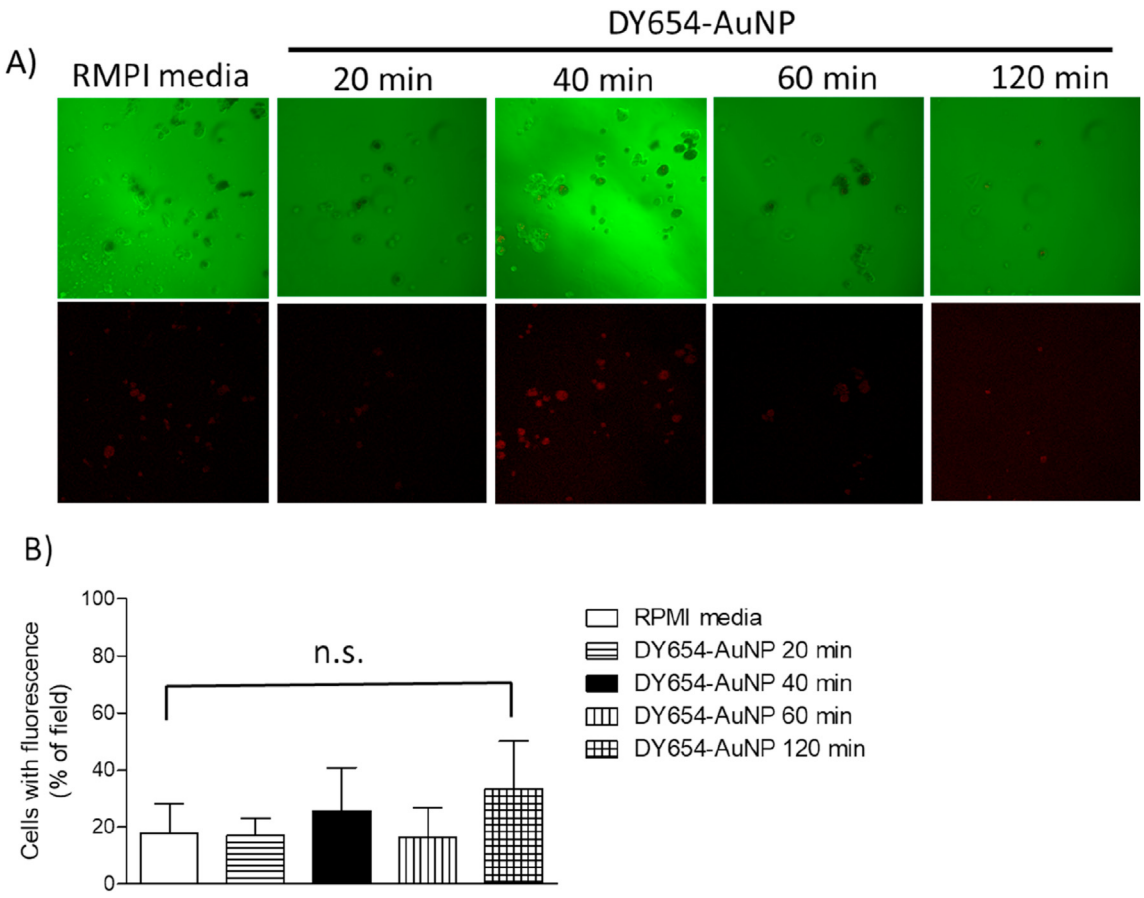

Figure 4. GL261 cells uptake of fluorescent DY654 covered gold nanoparticles (DY654-AuNP). A) Representative images of GL261 cells in presence of DY654-AuNP or RPMI medium. Images were captured 20, 40, 60 or 120 min after adding the DY654-AuNP solution to the cell culture medium. B) Quantification of the fluorescent cells (in % of field). There was no difference in percentage of fluorescent cells in any time tested ($P > 0.05$). One-way ANOVA was used as statistical test. Results are the average of three different assays. Not significant, n.s.

glioblastoma cell lines, particularly: U87, U87-EGFRvIII, U251, T98G, or U138 [38, 39, 40]. Absence of gold nanoparticles effects on tumor cells growth may come from their low uptake into the cells. In fact, we observed no important penetration of DY654-AuNP into the GL261 cells. Similar result was reported by BHAMIDIPATI & FABRIS [41] who demonstrated negligible uptake of PEG-AuNP by U87 glioma cell line and fibroblasts. Some factors like the gold nanoparticle covering and the type of tumor cell are known to influence the nanoparticle uptake. Corroborating with that, it was demonstrated that polyethylene imine (PEI)/-fluorescein isothiocyanate (FITC)-covered gold nanoparticles were up to 80% internalized by JHH520, JHH407 and GBM1 glioblastoma stem cells lines. The uptake rate varied though depending on the cell type [42]. In the same way, dithiolated diethylenetriaminepentaacetic acid ultrasmall nanoparticles (4.5 nm in size) showed strong cell line dependence of the nanoparticle uptake, being higher in the glioblastoma U87-MG, pancreatic BxPC-3 and prostate PC-3 than in other cell lines [43]. Then, if an intracellular target is intended for a particular tumor cell, the gold nanoparticle covering must be carefully chosen.

Photothermal antitumor effect of gold nanoparticles has been widely described in animal models of GBM [44, 45]. The photothermal property of gold nanoparticles is due to the electron movement around the nanoparticle surface under near infrared light stimuli. This is called SPR [46]. Gold nanoparticles can also be used to carry drugs, interfering or silencing RNAs, or antibodies that target structures important for the full tumor growing. In fact, shrinkage of GBM was observed in GBM carrying rodents when spherical nucleic acids, consisting of a gold or lipid core surrounded by a layer of small interfering RNA (siRNA), micro RNA (miRNA), or antagonists, were used [47]. In the same way, cisplatin-carrying gold nanoparticles functionalized with a cell uptake peptide reduced the GBM size, but that reduction was not observed in the group treated with gold nanoparticles without cisplatin [48]. Using a chronic treatment with either cit-AuNP or anti-VEGF Ig covered-AuNP, we did not observe change in the GBM progression in mice. Furthermore, we did not observe alteration in the tumor volume after injecting anti-VEGF Ig by itself. Thus, reduction in the GBM progression after AuNP treatment may come from both the AuNP covering type, which can lead to greater BBB permeability, the AuNP surface area, which can allow enhanced number of antitumoral cargo, and/or the *in vivo* GBM experimental model used to test the gold nanoparticles effect. Further studies are needed to address this issue. Regarding to the VEGF antibody treatment, absence of long-acting effect of VEGF blockade reducing blood vessels, and consequently not changing glioblastoma multiforme volume, similar to our results, has largely been reported in the literature [49, 50].

Among the difficulties in treating the GBM, it is highlighted its infiltrative capacity, difficulty in identifying the tumor margins, presence of glioma stem cells, and the obstacle imposed by the BBB to the chemotherapy [51]. Then, trespass the BBB in a pharmacological concentration is important for reducing the GBM progression. However, as observed before for tumor cell internalization, nanoparticle covering may be of great importance to determine the number of nanoparticles that crosses the BBB. In fact, it was demonstrated that arginine-glycine-aspartic acid-like peptide decorated gold nanoparticles in brain tumor was 1.5-fold that of undecorated nanoparticles and 5-fold that of PEGylated nanoparticles [52]. Besides, the size of nanoparticles is also an important factor that influences the nanoparticle capacity of crossing the BBB. KANG *et al.* [53] demonstrated

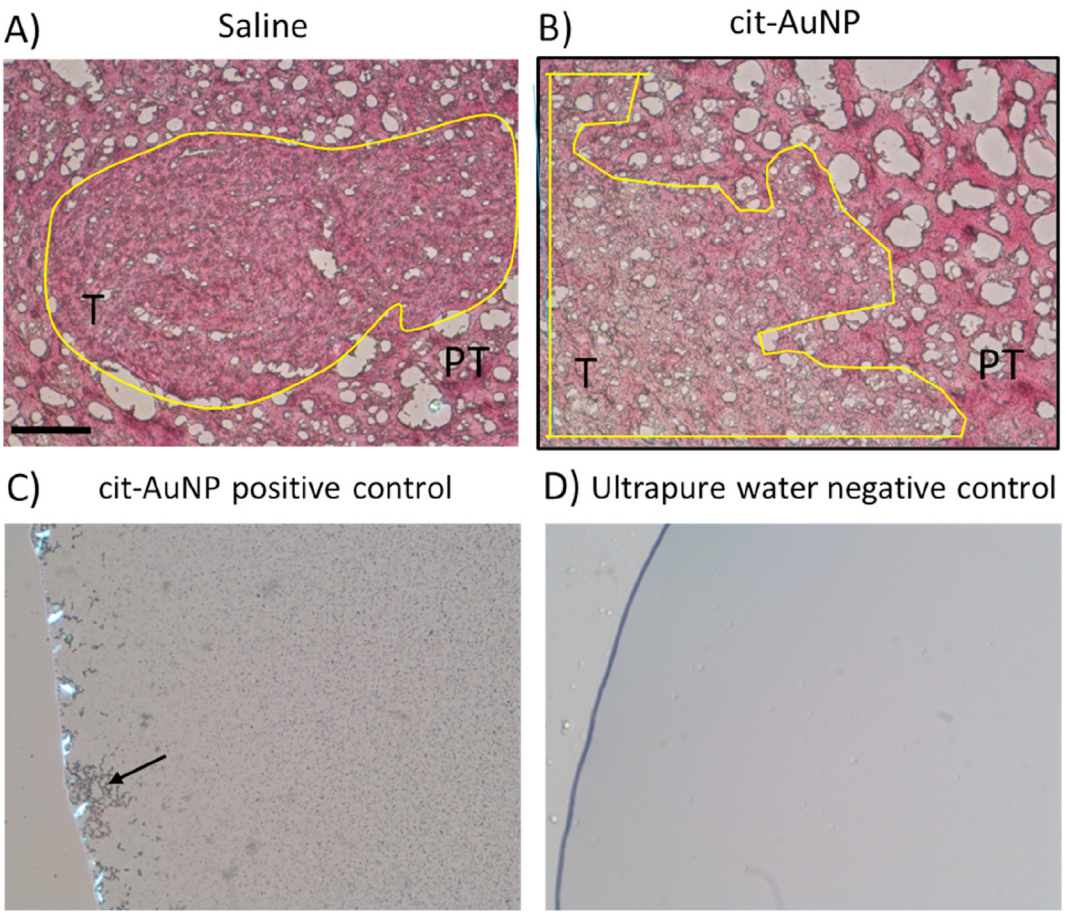

Figure 5. Gold visualization in tumoral (T) and peritumoral (PT) areas of brain slices obtained from glioblastoma multiforme (GBM)-carrying mice chronically treated with citrate-covered gold nanoparticles (cit-AuNP) or saline. Representative images of the cerebral tumor (yellow-circled) and peritumoral areas from GBM-carrying mice 24h after the last i.v. injection of saline (A) (control group) or cit-AuNP (B). No gold labelling was noticed in tumor and peritumoral cerebral areas from cit-AuNP-treated mice compared to the control group. In C, cit-AuNP and kit GoldEnhance reagent (Nanoprobes, Yaphank, NY, USA) positive control reaction carried out on a glass slide. Black tiny spots are spread all around the image and is highlighted by the large labeled black cluster the left side (black arrow). In D, ultrapure water served as negative control for gold labelling in which no black spot is noticed. Bar length = 100 μm.

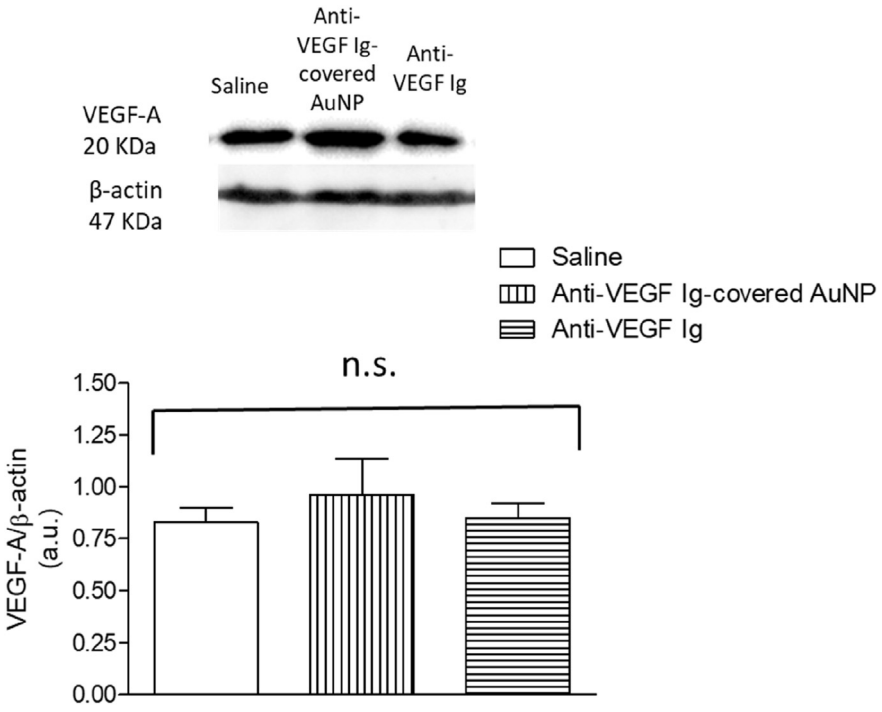

Figure 6. VEGF expression in cerebral glioblastoma multiforme (GBM)-carrying mice chronically treated with anti-VEGF Ig-covered gold nanoparticles (anti-VEGF Ig-covered AuNP), anti-VEGF Ig, or saline. Upper part: Representative images of VEGF and beta-actin blotting performed in cerebral GBM of mice 25 days after induction. |Animals were previously intravenously (i.v.) treated (chronically) with anti-VEGF Ig-covered AuNP, anti-VEGF Ig, or saline (control group). Lower part: Quantification of blotting in each group. No statistical difference was observed among groups ($P > 0.05$). Three animals per group were tested and comparison was made by using ANOVA. Results were normalized by the beta actin expression. Not significant, n.s. Arbitrary units, a.u.

that 10 nm fluorescent AuNP are found in the glioblastoma U87MG-induced tumor in mice, whereas 50 and 100 nm fluorescent AuNP were located only close to the blood vessels in the tumor. It was also reported that 3 nm glutathione-covered AuNP reached 73c murine glioma cells-induced glioma tumor thrice more than 18 nm glutathione-covered AuNP, even though those concentrations were dramatically lower than those observed in liver and spleen [54]. In the present study, we did not observe measurable presence of gold both in the GL261-induced GBM tumoral and peritumoral areas from the 20 nm cit-AuNP chronically treated mice. This result may explain the paralleled absence of effect of cit-AuNP chronic treatment in the GL261-induced GBM progression we observed. The same way, we did not observe change in the VEGF concentration into the tumor tissue in mice previously treated with the anti-VEGF Ig-covered AuNP, what reinforces these nanoparticles did not cross in appreciable amount the BBB to change the VEGF concentration into the tumor. In fact, VEGF adsorption to gold nanoparticles, even in absence of VEGF neutralizing antibody, was previously reported, *in vitro* [55]. Low tumor 22 nm PEG-AuNP entrance and short survival curve were also observed in mice carrying U251 cells-induced GBM [40]. Then, strategies to enhance the AuNP concentration in the glioblastoma and reduce the tumor size may include diminish the AuNP size, add different coverings, or include concomitant radiotherapy. In fact, it was demonstrated radiotherapy increases gold nanoparticles passage through the BBB, prolongs survival in mice carrying U251 glioma cells-induced tumor and enhances uptake of gold nanoparticles by tumor cells [40, 56]. Further studies are needed to determine the effect of radiotherapy along with 20 nm cit-AuNP chronic treatment in the GL261-induced GBM in mice.

5. Conclusions

In this article we demonstrated that either cit-AuNP or anti-VEGF Ig-covered AuNP is not a good option to treat GBM obtained after GL261 cells injection in brain parenchyma of mice. The lack of the antitumoral effect of gold nanoparticles was probably because they were not internalized in great number into the tumor cells or did not cross enough the BBB.

Declarations

Author contribution statement

S.F. Rodrigues: Conceived and designed the experiments; Performed the experiments; Analyzed and interpreted the data; Contributed reagents, materials, analysis tools or data; Wrote the paper.

V. Silva, R. Silva and L. Colli: Conceived and designed the experiments; Performed the experiments; Analyzed and interpreted the data.

M. Carvalho: Contributed reagents, materials, analysis tools or data.

Funding statement

This work was supported by Fundação de Amparo à Pesquisa do Estado de São Paulo (FAPESP), SP, Brazil (grant # 2014/05146-6; fellowships: # 2015/04281-0; # 2018/12368-6).

Declaration of interests statement

The authors declare no conflict of interest.

Additional information

Supplementary content related to this article has been published online at https://doi.org/10.1016/j.heliyon.2020.e05591.

References

[1] Q.T. Ostrom, H. Gittleman, G. Truitt, A. Boscia, C. Kruchko, J.S. Barnholtz-Sloan, CBTRUS statistical report: primary brain and other central nervous system tumors diagnosed in the United States in 2011–2015, Neuro Oncol. 20 (2018) iv1–86.

[2] H. Zong, L.F. Parada, S.J. Baker, Cell of origin for malignant gliomas and its implication in therapeutic development, Cold Spring Harb. Perspect. Biol. 7 (2015) a020610.

[3] J.H. Lee, J.E. Lee, J.Y. Kahng, S.H. Kim, J.S. Park, S.J. Yoon, et al., Human glioblastoma arises from subventricular zone cells with low-level driver mutations, Nature 560 (2018) 243–247.

[4] P. Wesseling, D. Capper, WHO 2016 Classification of gliomas, Neuropathol. Appl. Neurobiol. 44 (2018) 139–150.

[5] M. Cenciarini, M. Valentino, S. Belia, L. Sforna, P. Rosa, S. Ronchetti, et al., Dexamethasone in glioblastoma multiforme therapy: mechanisms and controversies, Front. Mol. Neurosci. 12 (2019) 65.

[6] D.T. Nagasawa, F. Chow, A. Yew, W. Kim, N. Cremer, I. Yang, Temozolomide and other potential agents for the treatment of glioblastoma multiforme, Neurosurg. Clin. N. Am. 23 (2012) 307–322.

[7] R. Stupp, W.P. Mason, M.J. Van Den Bent, M. Weller, B. Fisher, M.J. Taphoorn, et al., Radiotherapy plus concomitant and adjuvant temozolomide for glioblastoma, N. Engl. J. Med. 352 (2005) 987–996.

[8] R.L. Jensen, Brain tumor hypoxia: tumorigenesis, angiogenesis, imaging, pseudoprogression and as a therapeutic target, J. Neuro Oncol. 92 (2009) 317–335.

[9] L. Yang, C. Lin, L. Wang, H. Guo, X. Wang, Hypoxia and hypoxia-inducible factors in glioblastoma multiforme progression and therapeutic implications, Exp. Cell Res. 318 (2012) 2417–2426.

[10] N.A. Charles, E.C. Holland, R. Gilbertson, R. Glass, H. Kettenmann, The brain tumor microenvironment, Glia 59 (2011) 1169–1180.

[11] L.G. Dubois, L. Campanati, C. Righy, I. D'Andrea-Meira, T.C. Spohr, I. Porto-Carreiro, et al., Gliomas and the vascular fragility of the blood brain barrier, Front. Cell. Neurosci. 8 (2014) 418.

[12] R.K. Jain, E. Di Tomaso, D.G. Duda, J.S. Loeffler, A.G. Sorensen, T.T. Batchelor, Angiogenesis in brain tumours, Nat. Rev. Neurosci. 8 (2007) 610–622.

[13] N.Y. Frank, T. Schatton, M.H. Frank, The therapeutic promise of the cancer stem cell concept, J. Clin. Invest. 120 (2010) 41–50.

[14] W. Stummer, Mechanisms of tumor-related brain oedema, Neurosurg. Focus 22 (2007) E8.

[15] H.L. Wong, R. Bendayan, A.M. Rauth, Y. Li, X.Y. Wu, Chemotherapy with anticancer drugs encapsulated in solid lipid nanoparticles, Adv. Drug Deliv. Rev. 59 (2007), 491-404.

[16] L. Zhang, F.X. Gu, J.M. Chan, A.Z. Wang, R.S. Langer, O.C. Farokhzad, Nanoparticles in medicine: therapeutic applications and developments, Clin. Pharmacol. Ther. 83 (2008) 761–769.

[17] C.E. Mora-Huertas, H. Fessi, A. Elaissari, Polymer-based nanocapsules for drug delivery, Int. J. Pharm. 385 (2010) 113–142.

[18] W.J. Gradishar, S. Tjulandin, N. Davidson, H. Shaw, N. Desai, P. Bhar, et al., Phase III trial of nanoparticle albumin-bound paclitaxel compared with polyethylated castor oil–based paclitaxel in women with breast cancer, J. Clin. Oncol. 23 (2005) 77947803.

[19] C.L. Ventola, Progress in Nanomedicine: Approved and Investigational Nanodrugs, P.T. 42 (2017) 742–755. https://www.ncbi.nlm.nih.gov/pmc/articles/PMC5720487/pdf/ptj4212742.pdf.

[20] S. Wang, K.J. Chen, T.H. Wu, H. Wang, W.Y. Lin, M. Ohashi, et al., Photothermal effects of supramolecularly assembled gold nanoparticles for the targeted treatment of cancer cells, Angew. Chem. Int. Ed. 49 (2010) 3777–3781.

[21] M.K. Uchiyama, D.K. Deda, S.F. Rodrigues, C.C. Drewes, S.M. Bolonheis, P.K. Kiyohara, et al., In vivo and in vitro toxicity and anti-inflammatory properties of gold nanoparticle bioconjugates to the vascular system, Toxicol. Sci. 142 (2014) 497–507.

[22] E. Blacher, B. Ben Baruch, A. Levy, N. Geva, K.D. Green, S. Garneau-Tsodikova, et al., Inhibition of glioma progression by a newly discovered CD38 inhibitor, Int. J. Cancer 136 (2015) 1422–1433.

[23] S.M. Pyonteck, L. Akkari, A.J. Schuhmacher, R.L. Bowman, L. Sevenich, D.F. Quail, et al., CSF-1R inhibition alters macrophage polarization and blocks glioma progression, Nat. Med. 19 (2013) 1264–1272.

[24] A. Salazar-Ramiro, D. Ramírez-Ortega, V. Pérez De La Cruz, N.Y. Hérnandez-Pedro, D.F. González-Esquivel, J. Sotelo, et al., Role of redox status in development of glioblastoma, Front. Immunol. 7 (2016) 156.

[25] Y. Sanchez-Perez, E. Soto-Reyes, C.M. Garcia-Cuellar, B. Cacho-Diaz, A. Santamaria, E. Rangel-Lopez, Role of epigenetics and oxidative stress in gliomagenesis, CNS Neurol. Disord. - Drug Targets 16 (2017) 1090–1098.

[26] N. Dos Santos Tramontin, S. Da Silva, R. Arruda, K.S. Ugioni, P.B. Canteiro, G. De Bem Silveira, et al., Gold nanoparticles treatment reverses brain damage in alzheimer's disease model, Mol. Neurobiol. 57 (2020) 926–936.

[27] Y. Zheng, Y. Wu, Y. Liu, Z. Guo, T. Bai, P. Zhou, et al., Intrinsic effects of gold nanoparticles on oxygen-glucose deprivation/reperfusion injury in rat cortical neurons, Neurochem. Res. 44 (2019) 1549–1566.

[28] R.F. Araújo Jr., J.B. Pessoa, L.J. Cruz, A.B. Chan, E.C. Miguel, R.S. Cavalcante, et al., Apoptosis in human liver carcinoma caused by gold nanoparticles in combination with carvedilol is mediated via modulation of MAPK/Akt/mTOR pathway and EGFR/FAAD proteins, Int. J. Oncol. 52 (2018) 189–200.

[29] D. Coluccia, C.A. Figueiredo, M.Y. Wu, A.N. Riemenschneider, R. Diaz, A. Luck, et al., Enhancing glioblastoma treatment using cisplatin-gold-nanoparticle conjugates and targeted delivery with magnetic resonance-guided focused ultrasound, Nanomedicine 14 (2018) 1137–1148.

[30] E. Swanton, P. Savory, S. Cosulich, P. Clarke, P. Woodman, Bcl-2 regulates a caspase-3/caspase-2 apoptotic cascade in cytosolic extracts, Oncogene 18 (1999) 1781–1787.
[31] H. Li, H. Zhu, C.J. Xu, J. Yuan, Cleavage of BID by caspase 8 mediates the mitochondrial damage in the Fas pathway of apoptosis, Cell 94 (1998) 491–501.
[32] A.S. Dhillon, S. Hagan, O. Rath, W. Kolch, MAP kinase signalling pathways in cancer, Oncogene 26 (2007) 3279–3290.
[33] M. Patel, M.A. Vogelbaum, G.H. Barnett, R. Jalali, M.S. Ahluwalia, Molecular targeted therapy in recurrent glioblastoma: current challenges and future directions, Expet Opin. Invest. Drugs 21 (2012) 1247–1266.
[34] D. Allhenn, M.A. Boushehri, A. Lamprecht, Drug delivery strategies for the treatment of malignant gliomas, Int. J. Pharm. 436 (2012) 299–310.
[35] S.K. Baek, A.R. Makkouk, T. Krasieva, C.H. Sun, S.J. Madsen, H. Hirschberg, Photothermal treatment of glioma; an in vitro study of macrophage-mediated delivery of gold nanoshells, J. Neuro Oncol. 104 (2011) 439–448.
[36] D. Zhao, D. Alizadeh, L. Zhang, W. Liu, O. Farrukh, E. Manuel, et al., Carbon nanotubes enhance CpG uptake and potentiate antiglioma immunity, Clin. Cancer Res. 17 (2011) 771–782.
[37] S.F. Rodrigues, L.A. Fiel, A.L. Shimada, N.R. Pereira, S.S. Guterres, A.R. Pohlmann, et al., Lipid-core nanocapsules act as a drug shuttle through the blood brain barrier and reduce glioblastoma after intravenous or oral administration, J. Biomed. Nanotechnol. 12 (2016) 986–1000.
[38] Z. He, K. Liu, E. Manaloto, A. Casey, G.P. Cribaro, H.J. Byrne, et al., Cold atmospheric plasma induces ATP-dependent endocytosis of nanoparticles and synergistic U373MG cancer cell death, Sci. Rep. 8 (2018) 5298.
[39] L. Peng, Y. Liang, X. Zhong, Z. Liang, Y. Tian, S. Li, et al., Aptamer-conjugated gold nanoparticles targeting epidermal growth factor receptor variant III for the treatment of glioblastoma, Int. J. Nanomed. 15 (2020) 1363–1372.
[40] D.Y. Joh, L. Sun, M. Stangl, A.A. Zaki, S. Murty, P.P. Santoiemma, et al., Selective targeting of brain tumors with gold nanoparticle-induced radiosensitization, PloS One 8 (2013), e62425.
[41] M. Bhamidipati, L. Fabris, Multiparametric assessment of gold nanoparticle cytotoxicity in cancerous and healthy cells: the role of size, shape, and surface chemistry, Bioconjug. Chem. 28 (2017) 449–460.
[42] B. Giesen, A.C. Nickel, A. Garzón Manjón, A. Vargas Toscano, C. Scheu, U.D. Kahlert, et al., Influence of synthesis methods on the internalization of fluorescent gold nanoparticles into glioblastoma stem-like cells, J. Inorg. Biochem. 203 (2019) 110952.
[43] V. Ivošev, G.J. Sánchez, L. Stefancikova, D.A. Haidar, C.R. González Vargas, X. Yang, et al., Uptake and excretion dynamics of gold nanoparticles in cancer cells and fibroblasts, Nanotechnology 31 (2019) 135102.
[44] B. Seo, K. Lim, S.S. Kim, K.T. Oh, E.S. Lee, H.G. Choi, et al., Small gold nanorods-loaded hybrid albumin nanoparticles with high photothermal efficacy for tumor ablation, Colloids Surf. B Biointerfaces 179 (2019) 340–351.
[45] T. Fernandez Cabada, C. Sanchez Lopez De Pablo, A. Martinez Serrano, F. Del Pozo Guerrero, J.J. Serrano Olmedo, M. Ramos Gomez, Induction of cell death in a glioblastoma line by hyperthermic therapy based on gold nanorods, Int. J. Nanomed. 7 (2012) 1511–1523.
[46] A.M. Alkilany, L.B. Thompson, S.P. Boulos, P.N. Sisco, C.J. Murphy, Gold nanorods: their potential for photothermal therapeutics and drug delivery, tempered by the complexity of their biological interactions, Adv. Drug Deliv. Rev. 64 (2012) 190–199.
[47] S. Tommasini-Ghelfi, A. Lee, C.A. Mirkin, A.H. Stegh, Synthesis, physicochemical, and biological evaluation of spherical nucleic acids for RNAi-based therapy in glioblastoma, Methods Mol. Biol. 1974 (2019) 371–391.
[48] D. Coluccia, C.A. Figueiredo, M.Y. Wu, A.N. Riemenschneider, R. Diaz, A. Luck, et al., Enhancing glioblastoma treatment using cisplatin-gold-nanoparticle conjugates and targeted delivery with magnetic resonance-guided focused ultrasound, Nanomedicine 14 (2018) 1137–1148.
[49] J.L. Li, R.C. Sainson, C.E. Oon, H. Turley, R. Leek, H. Sheldon, et al., DLL4-Notch signaling mediates tumor resistance to anti-VEGF therapy in vivo, Cancer Res. 71 (2011) 6073–6083.
[50] K. Angara, T.F. Borin, M.H. Rashid, I. Lebedyeva, R. Ara, P.C. Lin, et al., CXCR2-Expressing tumor cells drive vascular mimicry in antiangiogenic therapy-resistant glioblastoma, Neoplasia 20 (2018) 1070–1082.
[51] S. Pinel, N. Thomas, C. Boura, M. Barberi-Heyob, Approaches to physical stimulation of metallic nanoparticles for glioblastoma treatment, Adv. Drug Deliv. Rev. 138 (2019) 344–357.
[52] B. Albertini, V. Mathieu, N. Iraci, M. Van Woensel, A. Schoubben, A. Donnadio, et al., Tumor targeting by peptide-decorated gold nanoparticles, Mol. Pharm. 16 (2019) 2430–2444.
[53] J.H. Kang, J. Cho, Y.T. Ko, Investigation on the effect of nanoparticle size on the blood-brain tumour barrier permeability by in situ perfusion via internal carotid artery in mice, J. Drug Target. 27 (2019) 103–110.
[54] C. Peng, X. Gao, J. Xu, B. Du, X. Ning, S. Tang, et al., Targeting orthotopic gliomas with renal-clearable luminescent gold nanoparticles, Nano Res. 10 (2017) 1366–1376.
[55] Y. Zhang, X. Xiong, Y. Huai, A. Dey, M.N. Hossen, R.V. Roy, et al., Gold nanoparticles disrupt tumor microenvironment - endothelial cell cross talk to inhibit angiogenic phenotypes in vitro, Bioconjugate Chem. 30 (2019) 1724–1733.
[56] F. Kazmi, K.A. Vallis, B.A. Vellayappan, A. Bandla, D. Yukun, R. Carlisle, Megavoltage radiosensitization of gold nanoparticles on a glioblastoma cancer cell line using a clinical platform, Int. J. Mol. Sci. 21 (2020) 429.